{Draft} Design Proposal: Mach Zehnder Interferometer

1[st] edx Username - Nsanebolt9

***Abstract*—Abstract loading...**

***Index Terms*—Silicon Photonics, Mach-Zender Interferometer, Group Index, Free Spectral Range**

I. Introduction

Photonics is an exciting field that continues to gain traction over the years. It has already been largely incorporated into data centers with growing development in quantum computing, biomedical applications, and sub-wavelength silicon photonics. This course provides both beginners and advanced engineers a platform to study and research the world of silicon photonics.

One collective device the course focus on is the Mach-Zehnder Interferometer (**MZI**) fabricated on a silicon wafer. Building a foundation with a pinnacle group is important when branching further into the field of sub-wavelength photonics. A structured approach to understanding different components for waveguide modes, structure, propagation loss, couplers, and gratings.

This report focuses on an unbalanced passive MZI with different path lengths (Δ**L**). We will show how different path lengths could affect Free Spectral Range (**FSR**) and loss based on arm design.

II. Theory

We begin by breaking down the theory and structure of MZI behaviors, as seen in Fig 1. Light will be supplied to one grating coupler, where the light will begin propagating through our silicon waveguide. The cross section of the waveguide, Fig. 2, will guide the light along the silicon path. For this class, we focus on waveguide height and width of 200×500 nm. The structure of this waveguide can guide two modes, TE_1 and TM_1. This report will only focus on TE_1 mode.

As light travels through the device, the output electric field, E_o, depends on the input electric field,

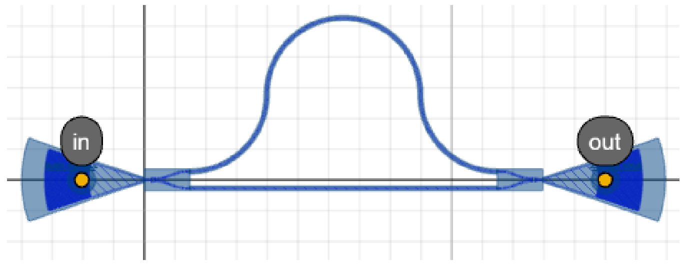

(a) Structure

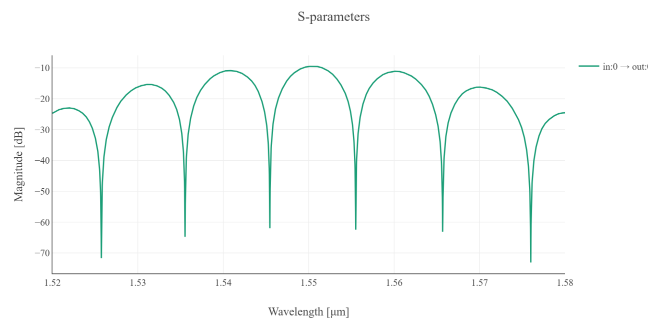

(b) FSR

Fig. 1: Structure and behavior expectation for MZI simulated using IPKISS software [1].

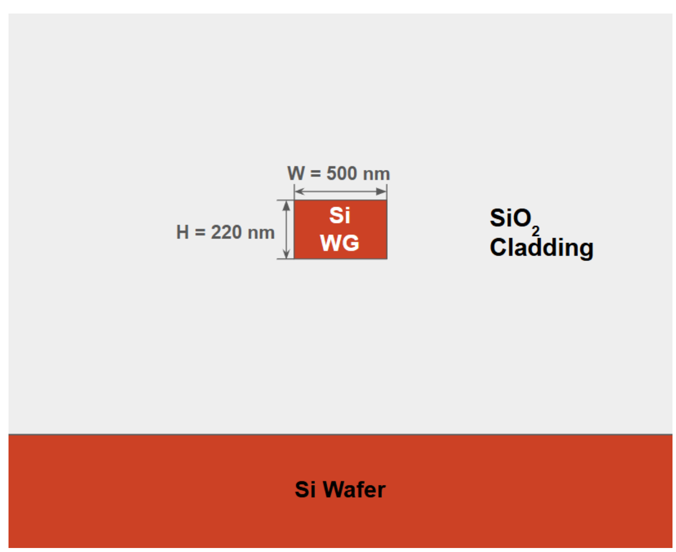

Fig. 2: Cross section of a silicon waveguide with SiO_2 cladding used in this report. With dimensions 500 nm x 220 nm.

E_i, the difference in the path $\Delta L = L_2 - L_1$, and the propagation, β, as,

$$E_o = \frac{E_i}{\sqrt{2}}(e^{-i\beta L_1} + e^{-i\beta L_2}). \tag{1}$$

The propagation of light through the waveguide is a function of wavelength as $\beta = \frac{2\pi\, n_{eff}(\lambda)}{\lambda} + i\frac{\alpha}{2}$ where α is the propagation loss and is dependent on waveguide dimension.

This brings us to define the light intensity as the transfer function,

$$T_{MZI}(\lambda) = \frac{1}{4}\left|e^{-i\beta L_1} + e^{-i\beta L_2}\right|^2 \tag{2a}$$

$$= \frac{1}{4}\left|1 + e^{i\beta(\lambda)\Delta L}\right|^2. \tag{2b}$$

Defining the FSR for an interferometer is a great way to characterize the structure efficiency and working range. It is defined as,

$$FSR = \frac{\lambda^2}{\Delta L n_g}, \tag{3}$$

where n_g the group index. We can re-arrange the above equation as,

$$n_g = \frac{\lambda^2}{\Delta L\ FSR}. \tag{4}$$

We can use this and multiple unbalanced MZI's to determine the group index of our fabricated design. This allows us to compare the accuracy of the simulated device, but also the fabrication capabilities, as we will discuss later.

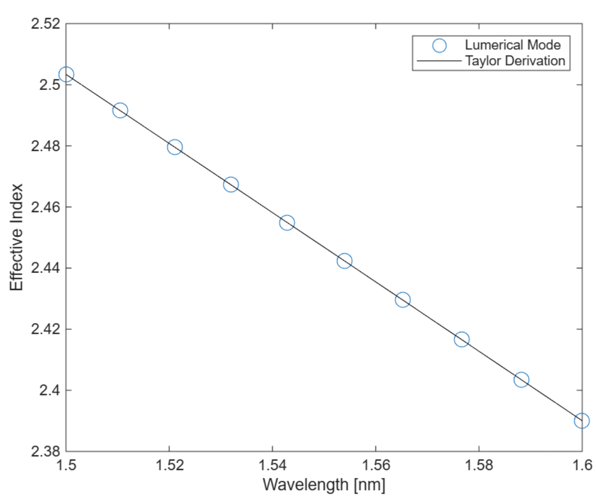

Fig. 3: 2nd order Taylor Series for compact model. Derived equation in Eq.6

Currently we can compare a simulated model using Lumerical MODE versus the Taylor Series equation derived in the course for effective index. The compact model of the effective index using a Taylor expansion format. We arrive to,

$$n_{eff}(x) = n_1(x) + n_2(x) \times (\lambda - \lambda_0) + n_3(x) \times (\lambda - \lambda_0)^2, \tag{5}$$

where the center wavelength, λ_0, in our experimental set-up is 1.55 μm.

Using MATLAB we can solve for $n_1(x)$, $n_2(x)$, and $n_3(x)$ based on a simulation set-up at the center wavelength extracted from Lumerical Mode. This was done for practice in *Waveguide Modeling - Lumerical Mode* section. Using MATLAB, the following was derived for a central wavelength of $\lambda_0 = 1.55$ μm,

$$n_{eff}(x) = 2.45 - 1.13(\lambda - 1.55) - 0.04(\lambda - 1.55)^2, \tag{6}$$

also seen in Fig 3.

III. Modeling and Simulation

Next, we can discuss the simulated data extracted from Lumerical MODE used for the compact effective index model in Eq. 6. As mentioned earlier, the waveguide dimension allows two modes to propagate, as seen in Fig. 4 and characterized in Table I. As we learned in the course, effective index and group index are dependent on wavelength. We simulated this using Lumerical MODE's Eigensolver. The wavelength sweep is shown in Fig. 5. We used this data with MATLAB to help define Eq. 6 and produce Fig. 3.

TABLE I: Model effective and group index's at a wavelength of 1.55 μm for a waveguide dimension of 0.5×0.22 μm.

Mode	Effective Index (n_{eff})	Group Index (n_g)	Propagation Loss (α) [dB/cm]
TE_1	2.44	4.20	4.4×10^{-4}
TM_1	1.77	3.74	3.0×10^{-4}

A. Proposed Design

Current draft of MZI structure layout seen in Fig. 6 and listed in Table II. Luceda IPKISS was also used to simulate experimental FSR and loss, as seen in Fig. 7.

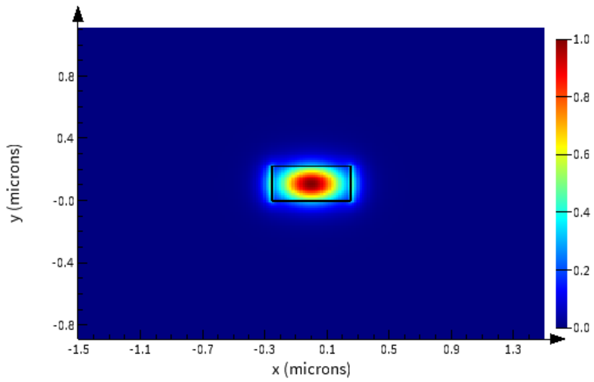

(a) TE

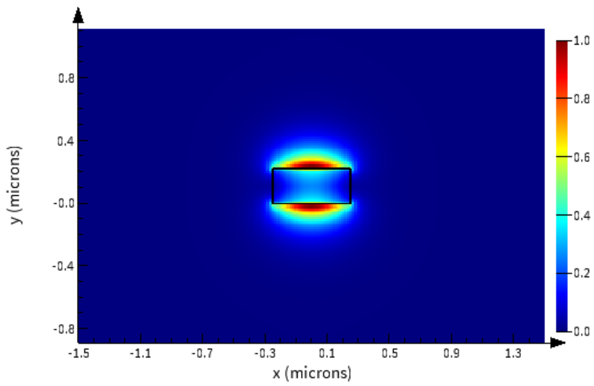

(b) TM

Fig. 4: Simulated waveguide mode profile using Lumerical MODE Solution.

TABLE II: Expected results for Designs.

Design #	Waveguide Width (μm)	Path Length Difference (μm)	FSR (nm)	Loss (dB)
1	0.5	30	19.1	11.4
2	0.5	40	14.3	9.4
3	0.5	60	9.5	9.5
4	0.5	80	7.2	9.5
5	0.5	100	5.7	9.5
6	0.5	120	4.8	9.8
7 ($r=20.4\mu$m)	0.5	46.5	12.3	9.5
8 ($r=10.2\mu$m)	0.5	46.5	12.3	9.5
9 ($r=6.8\mu$m)	0.5	46.5	12.3	9.5
10 ($r=5.1\mu$m)	0.5	46.5	12.3	9.5
11 (control)	0.5	46.5	12.3	9.5

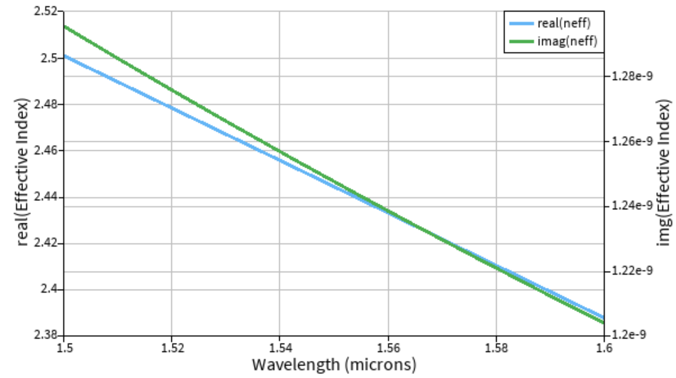

(a) Effective Index

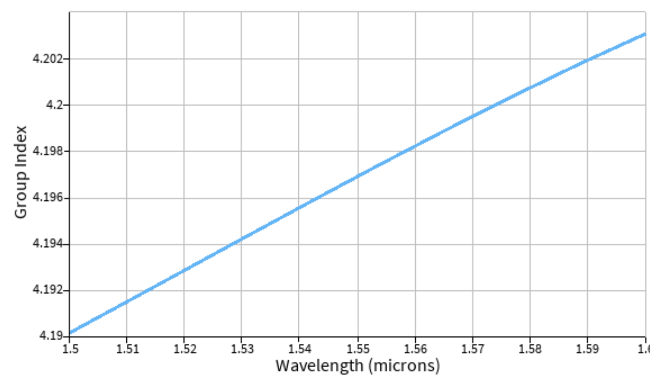

(b) Group Index

Fig. 5: Lumerical mode index simulation results.

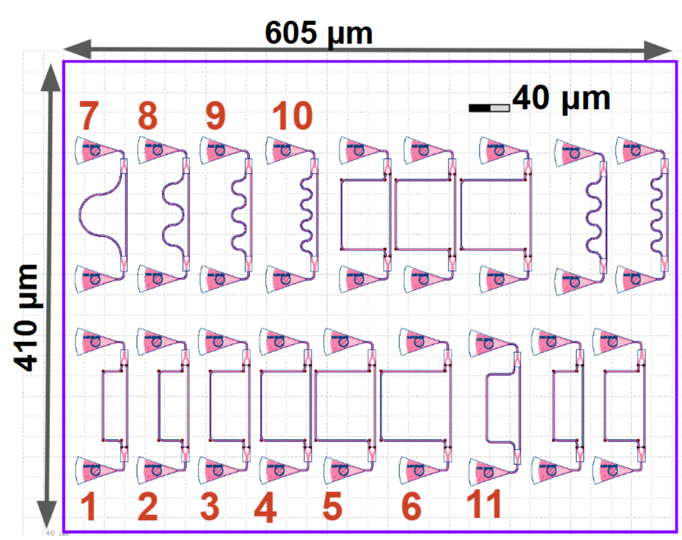

Fig. 6: Draft design for devices with ΔL: **(1)** 30 μm, **(2)** 40 μm, **(3)** 60μm, **(4)** 80 μm, **(5)** 100 μm, **(6)** 120 μm, and **(7-11)** 46.5 μm. Rough surface dimension of 605×410 μm.

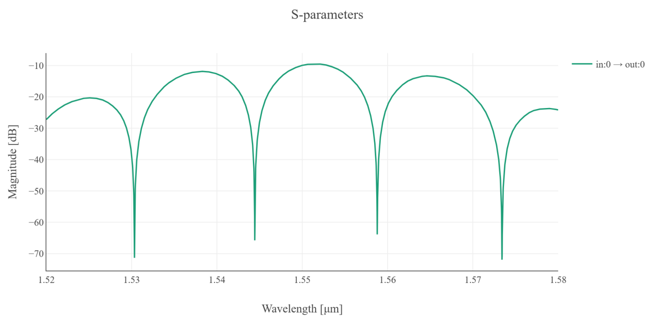

(a) $\Delta L = 40\ \mu$m

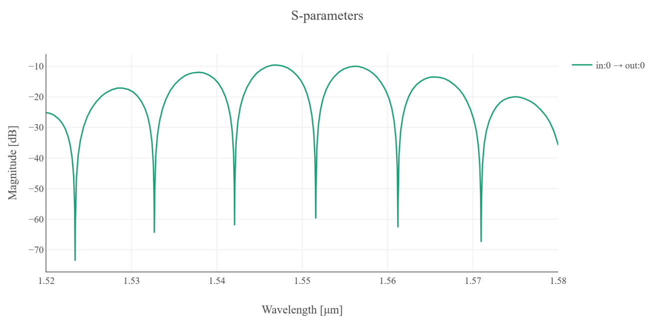

(b) $\Delta L = 60\ \mu$m

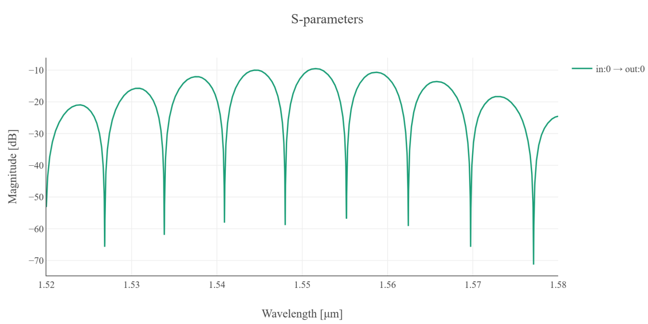

(c) $\Delta L = 80\ \mu$m

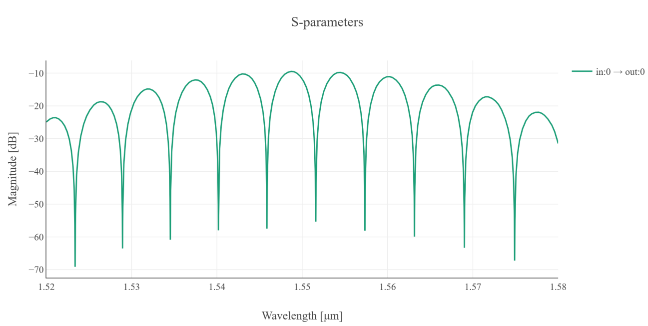

(d) $\Delta L = 100\ \mu$m

Fig. 7: Free Spectral Range for Mach-Zehnder Interferometer with different path lengths ΔL.

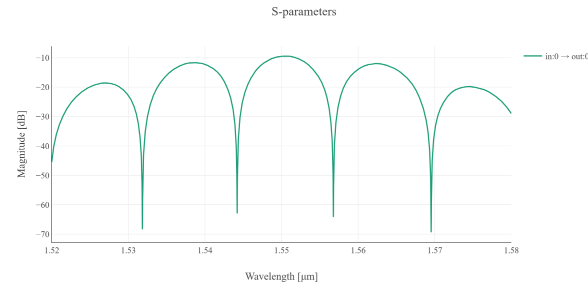

Fig. 8: Free Spectral Range for multi-bend Mach-Zehnder Interferometer with path lengh of 46.5 μm.

IV. Fabrication

Fabrication Loading...

Sed feugiat. Cum sociis natoque penatibus et magnis dis parturient montes, nascetur ridiculus mus. Ut pellentesque augue sed urna. Vestibulum diam eros, fringilla et, consectetuer eu, nonummy id, sapien. Nullam at lectus. In sagittis ultrices mauris. Curabitur malesuada erat sit amet massa. Fusce blandit. Aliquam erat volutpat. Aliquam euismod. Aenean vel lectus. Nunc imperdiet justo nec dolor.

V. Analysis

Analysis Loading...

Sed feugiat. Cum sociis natoque penatibus et magnis dis parturient montes, nascetur ridiculus mus. Ut pellentesque augue sed urna. Vestibulum diam eros, fringilla et, consectetuer eu, nonummy id, sapien. Nullam at lectus. In sagittis ultrices mauris. Curabitur malesuada erat sit amet massa. Fusce blandit. Aliquam erat volutpat. Aliquam euismod. Aenean vel lectus. Nunc imperdiet justo nec dolor.

VI. Conclusion

This report breaks down the characteristics of a sub-micron silicon photonics unbalanced MZI device. By simulating and constructing an MZI, it provides a foundation to experimental curiosity. The proposal showed the basic breakdown on how to analyze and determine system parameters.

References

[1] Lucedia IPKISS Software. https://www.lucedaphotonics.com/luceda-photonics-design-platform

[2] edx-SiEPIC Course Slides, https://learning.edx.org/course/course-v1:UBCx+Phot1x+1T2026/home.

[3] KLayout Software. http://www.klayout.de

[4] Ansys Lumerical MODE Software. https://www.ansys.com/products/optics/mode